Restitution of Longwave and Shortwave radiative fluxes at the top of the atmosphere from combination of ScaRaB and METEOSAT data.

Michel Viollier

LMD, Ecole Polytechnique, 91128 Palaiseau Cedex, France

MEGHA-TROPIQUES 2nd Scientific Workshop, 2-6 July 2001, Paris, France.

Abstract

Comparison between ScaRaB and METEOSAT is useful to adjust the METEOSAT calibration but also to provide empirical conversion between narrow-band METEOSAT radiances and fluxes. We have studied the combination of METEOSAT-5 and ScaRaB/Resurs during INDOEX 1999. The study includes several issues: to co-register both sets of data, to compare the estimated narrow band METEOSAT radiances to the broadband ScaRaB radiances, to converse radiances to fluxes as a function of the observation angles. In the longwave domain, multiple regression has been used between the ScaRaB flux, the two infrared METEOSAT channels (infrared window and water vapor channel) and the zenith view angle. The root-mean-square errors based on these fits are of the order of less than 10 Wm^{-2}. The conversion equation has been used to extrapolate the two-per-day ScaRaB fluxes to each half-hour METEOSAT observations. In the SW domain the comparisons are much more difficult. First the observations are more sensitive to clouds, making more critical the co-registration procedure. Secondly the anisotropy of the radiation field is more marked. After narrow-to-broadband radiance conversion and angular ERBE-based corrections the mean error (rms.) is of the order of 40 Wm^{-2} on the flux retrieval. A large part of differences comes from the co-registration errors and from the narrow-to-broad conversion. Further studies are necessary to reduce not only the rms. errors but also the individual errors, thanks to improved co-registration method, to new angular dependence models and to a better scene identification using the high METEOSAT spatial resolution.

1. Introduction

The attempt to retrieve the SW and LW fluxes from METEOSAT-5 is a component of the MeghaTropiques studies. The views are to increase the temporal sampling of flux estimations and to merge imager and large FOV instrument in order to get a better scene identification. This project requires comparisons with flux estimated by Earth Radiation Budget (ERB) instrument such as ScaRaB (Kandel et al., 1998). ScaRaB provides not only well calibrated radiances (better than 2%) and but also estimated fluxes in both the shortwave and longwave domains. The comparison is then useful to adjust the Meteosat calibration (not better than 5% in the SW) and also to provide empirical conversion between narrow-band Meteosat radiances and fluxes. Fluxes (albedo and outgoing longwave radiation) are essential characteristics for the role of clouds in meteorology and climate. During the INDOEX experiment, from January 20 to the end of March 1999, about 50 days of ScaRaB-2 data (Duvel et al., 2001) are available and can be compared to METEOSAT-5 data. The present study is based on this dataset.

To fulfil the same objectives, previous studies have already been carried out using different couples of instruments, for example: ERBE and Meteosat (Cheruy et al, 1991, Vesperini and Fouquart, 1994) , ERBE and GOES (Minnis et al, 1991), ScaRaB and Meteosat (Dewitte et al, 1999), ScaRaB and GOES (Li and Trischenko, 1998, 1999, Trischenko and Li, 1998). The following table summarizes some results. Most of these studies deal with small subsets of data (i.e. one orbit to some days) whereas we intend here to compare almost three months of data.

Author	Comments	rms difference LW Wm^{-2}	rms difference SW Wm^{-2}
Cheruy et al, 1991 ERBE Meteosat	Flux = Flux (IR, WV)	10	
Vesperini and Fouquart, 1994, ERBE Meteosat	Flux SW		41.1
Dewitte et al, 1999 ScaRaB1-Meteosat same	Radiance.x π central point	18	80
	Radiance x π PSF convolution	17	37
Trishchenko and Li, 1998 ScaRaB GEOS	Flux, VZA < 25°		29

Table 1 – Some comparisons between imaging and ERB fluxes in the LW and SW domains (PSF = point spread function VZA = View Zenith Angle).

One observes that the rms errors is larger is in the SW than in the LW. This is due to the spatial and temporal variability of the SW radiation field and also because the anisotropy of the radiation field is more marked in the SW. Second remark: the differences strongly depend whether the METEOSAT data are averaged or not over the ScaRaB footprint. These two points will be further discussed in our study.

2. Data and Methods

2.1. Satellite data

On board RESURS (Duvel et al, 2001) the ScaRaB instrument is a cross-track scanning radiometer with a swath of about 1800 km giving gaps from one orbit the next near the equator (figure 1). The RESURS orbit is sun-synchronous with the ascending node at the Equator at 22:30. ScaRaB has an onboard calibration system using multiple sources (blackbody simulators and three sets of lamps). Calibration procedures use also geophysical cross-calibration between the total and SW channels (Duvel and Raberanto, 2000). The estimated calibration uncertainty is in the order or less than 2% (1% in the LW). Coincident and collocated CERES and ScaRaB observations have also been found consistent to within 0.5% and 1.5% in the LW and SW domain respectively (Haeffelin et al, 2001).

METEOSAT like other imaging radiometers of meteorological are first designed to make pictures of cloud pattern and accurate absolute calibration was not emphasized. Infrared calibration is provided but the reference blackbody, on board METEOSAT cannot be monitored through the complete optical system. There is no onboard calibration system for the visible, so only a posteriori vicarious calibration is available, probably not better than 5% (Brest et al, 1997). Meteosat has 3 channels: visible (0.3-1.1μm), infrared window (IR) (10.5-12.5 μm) and water vapor (WV) (5.7-12.5 μm). The advantages of METEOSAT are the excellent spatial and temporal sampling: we have used the 'full resolution' Meteosat data set (5km) specifically prepared by LMD (J.L. Monge, Climserv data base) for INDOEX. These Meteosat data are available each half-hour (figure 3). We have limited our study to the area: 30°E, 110°E, 35°S, 35°N.

2.2. Search for simultaneous observations

Only the ScaraB observations occurring during the METEOSAT image generation are retained, meaning the time difference is less than 20 minutes. Figure 1 and table 2 explain the successive occurrences of simultaneous ScaRaB and METEOSAT measurements. The ScaRaB orbit over the Bay of Bengal or Eastern Africa are simultaneous with respectively METEOSAT slots 10 (04:00) and 16 (07:30).

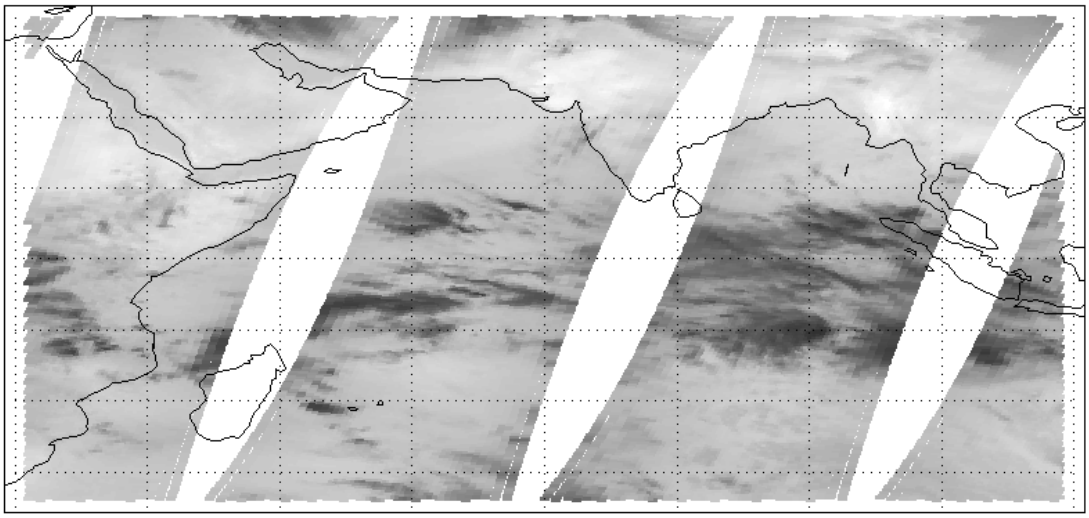

Fig. 1 Coverage of 4 successive ScaRaB orbits (3581 to 3584) over the INDOEX area on March 19, 1999.

Meteosat Image In the day (1-48)	Meteosat UTC	ScaRaB Orbit	ScaRaB Location
10	04:30 05:00	3582	Bay of Bengal
13	06:00 06:30	3583	Arabian Sea
16	07:30 08:00	3584	Eastern Africa
31	15:30 16:00	3582-3583	Indonesia
35	17:00 17:30	3589-3590	India
38	18:30 19:00	3590-3591	Arabia

Table 2 Major synchronous collocations on March 19 1999. The three first lines correspond to daytime (figure 1), the last to nighttime.

2.3. Collocation

The difference in spatial resolutions of the two systems (>40km for ScaRaB, 5 km and 2.5 km for METEOSAT) require that for each ScaRaB pixel, the surface area corresponding to the ScaRaB pixel area is calculated and converted into corresponding METEOSAT lines and pixels of which the average value is used. The convolution with the point spread function (Dewitte et al, 1999) should be used instead of simple average. These computations are too complex and time-consuming to be applied to our huge data set. In a first attempt we have averaged the radiances over an area comparable to the ScaRaB/RESURS footprint (50 km at nadir, >80 km at the edges). According to the METEOSAT resolution (5km for IR, 2.5 km for VIS) we first have averaged over square of 7x7 (LW), 19x19 (SW). In the SW domain we then have tried different size of the averaging area (table 3). It can be seen that small areas give the poorest correlation (comparable to the central pixel case in table 1). The optimum is obtained for large areas (60 km).

METEOSAT Averaging area (km)	SW ScaRaB-METEOSAT SW-VIS comparisons regression coefficient R
7.5 x 7.5	0.86
32 x 32	0.90
42 x 42	0.910
48 x 48	0.914

62 x 62	0.930
150 x 150	0.926

Table 3 Impact of the size of the averaging area on regression between SW (ScaRaB) and VIS radiances.

2.4. Differences in geometry of view

The observation angles of ScaRaB and METEOSAT are totally different depending on their distance to the Earth (36000 km vs 820 km). From a geostationary satellite a given area of the Earth is always observed with the same view zenith angle (VZA). On the contrary due to the orbit shift from one day to the next day the view angles of a polar satellite constantly change. The radiance depends on this angle, specifically in the SW domain, where the reflected radiation depends on the relative position of the observation and of the incidence of the Sun's ray (sun zenith angle -SZA and relative azimuth angle-RAA). Computed from VZA, SZA and RAA, two angles play a major role in the anisotropy of the reflected radiation: γ the scattering angle and α the angle from the line of specular reflection. The most obvious aspect of the SW anisotropy is the sun glint over the ocean, which is observed when, α is close to zero. This α angle has been computed for the METEOSAT observations coincident with ScaRaB (figure 2a). One concludes that, for these points, the sun glint is mainly observed in the Bay of Bengal. The Eastern Africa seen on the third orbit of ScaRaB is observed 3 hours after: with the same VZA (fixed METEOSAT geometry), the same mean SZA (due to the ScaRaB sun-synchronism), but with a different RAA which yields a larger α and then no sun glint. This is observed on the corresponding three slots of METEOSAT (figure 3). The α angle is shown for the ScaRaB geometry on figure 2 b: the sun glint then arise in the eastern part of the scan. These two figures illustrate that our coincident and collocated points are observed with totally geometry of view relatively to the Sun incidence. In major part of cases the two instruments then settle different aspects of the anisotropy of the reflected flux. Radiances are comparable if only the observation angles are almost identical, which occurs only on a few cases.

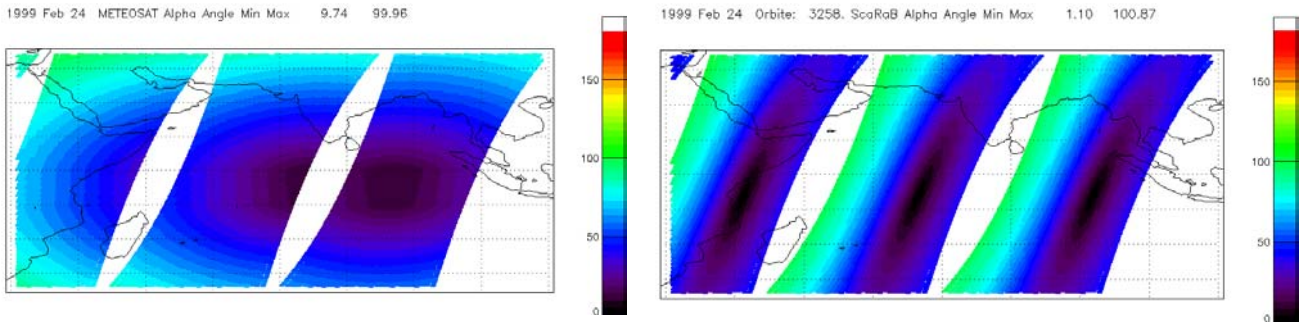

Fig. 2 Angle from the line of specular reflexion (sun glint) for (a) Meteosat, data coincident with ScaRaB, and (b) for ScaRaB

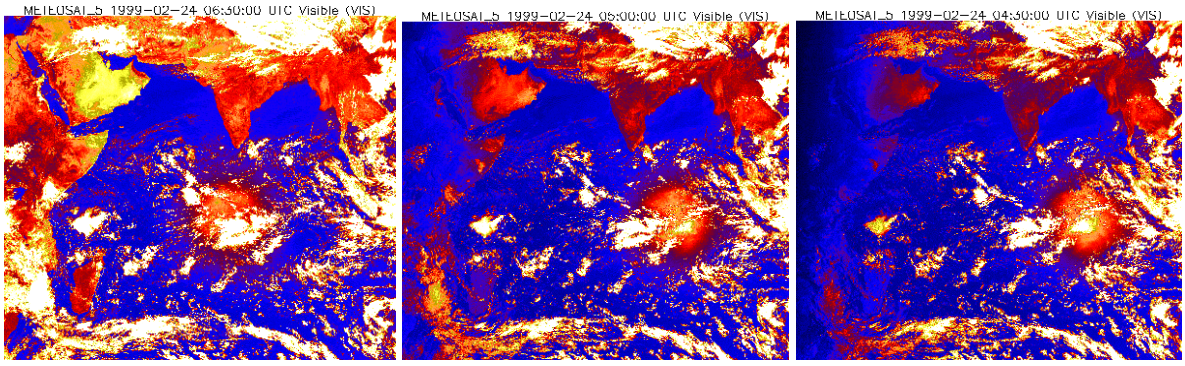

Fig. 3 METEOSAT VIS data, at 06:00(a), 05:00(b) and 04:00(c). The color scale (blue-red-orange-yellow-white) is the same for the 3 figures and it has been adjusted to emphasize the sun glint (the orange slot below white cloud pattern). The sun glint is shifted westerly from c to a.

3. Results

3.1. LW Domain

With objectives and data similar to this study, and using simultaneous collocated Meteosat (23/11/1984) with Meteosat 2 (located at 0°, 0°), and ERBE data, Cheruy et al, (1991) found regression for estimating the flux from the infrared (IR) and water vapor (WV) radiances with rms errors of the order of less than 10 Wm^{-2}. The best results were obtained with the following equation

$$Flux = A0 + A1.IR + A2.IR^3 + A3.IR/\cos(zen) + A4.WV + A5.WV^2 \qquad (1)$$

where zen is the viewing zenith angle and accounts for the limb darkening effect.

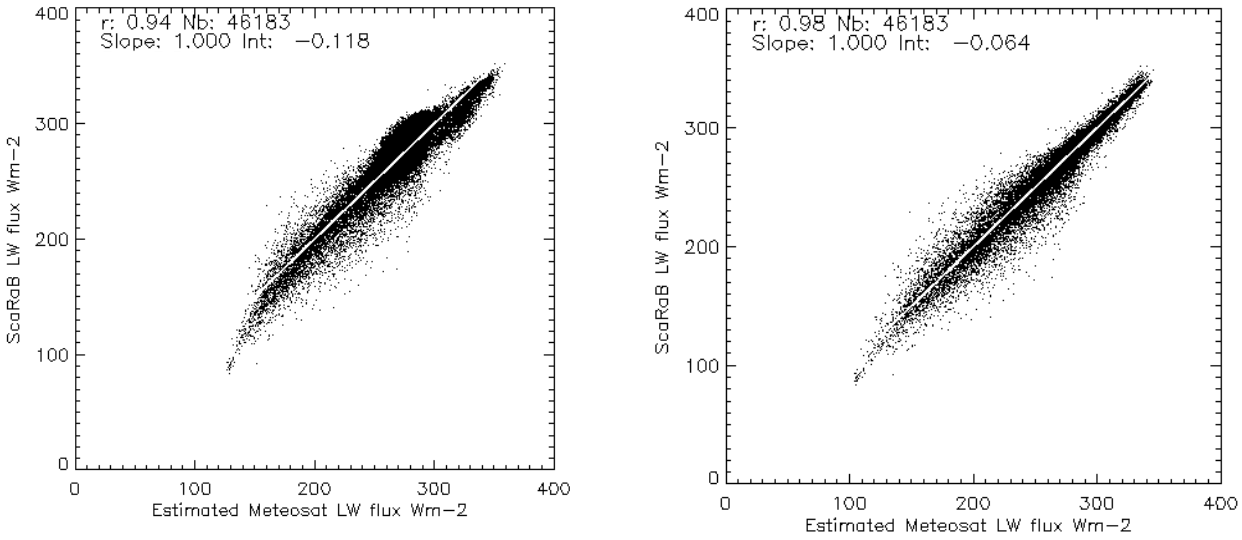

Fig. 4 Correlations using (a) simple linear regression (canal IR) and (b) full regression (IR+WV)

The same multiple regression has here been applied to the ScaRaB/METEOSAT-5 collocated and near-simultaneous dataset. The following coefficients have been found:

A0=65.479 ; A1=14.192 ; A2=-0.0079 ; A3=1.8412 ; A4 = 61.33 ; A5=-11.03

Corresponding to 620 800 individual data from January to March 1999 (figure 7b). The regression coefficient is R^2=94.1 and the rms error 9.45 Wm^{-2}.

Corresponding to a subset of data, figure 4 clearly shows the improvement between a simple one-channel linear regression and the multiple regression including the IR and WV channels.

The equation 1 with the listed coefficients has been used by Roca et al (2001).

3.2. SW Domain

3.2.1. Radiance Conversion

In a first attempt the comparisons of the SW and VIS radiances of ScaRaB and METEOSAT (figure 5a) shows a large scattering. In a second attempt (figure 5b) the scattering is reduced by eliminating the sun-glint data. This elimination is based on geometrical computations (see figure 2a), the threshold of the glint angle being here fixed to 20°. The near-nadir observations are then expected to be spoiled by sun glint since the major part of the INDOEX subset covers the ocean. To avoid this problem, the radiance calibration have been searched from VZA greater than 30° (figure 6) and same RAA and VZA (difference not greater than 20°). From this figure, the formula of radiance calibration and of narrow-to-broadband conversion as a function of the visible numerical count (CN) is then

$$R_{sw,Meteosat} = 1.4113\ NC + 6.647 \qquad (2)$$

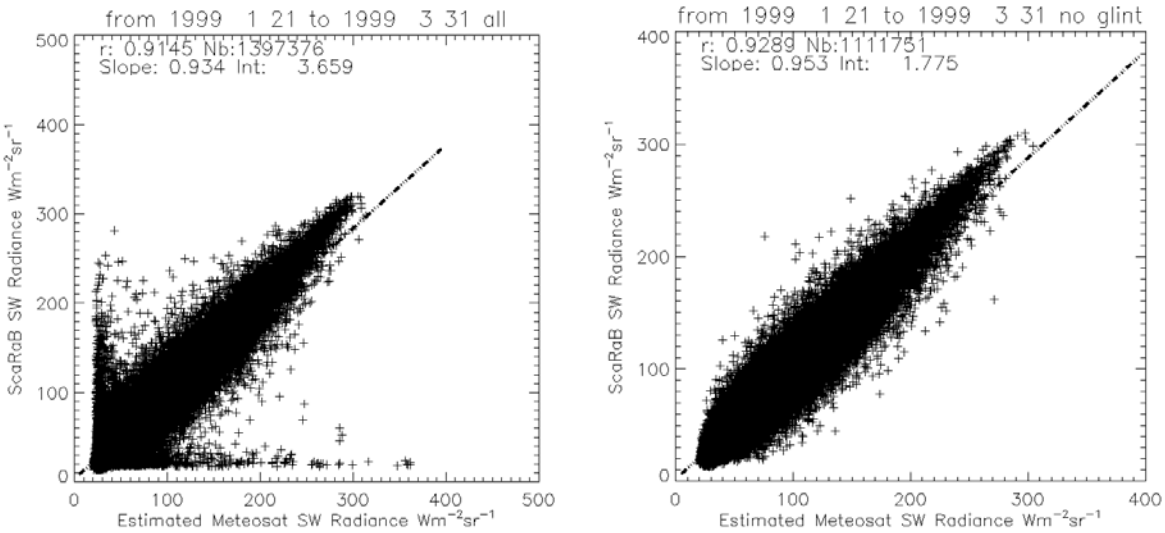

Fig. 5 Correlations between SW ScaRaB and VIS METEOSAT Radiances using (a) all collocated observations and (b) all except 'sun glint' areas

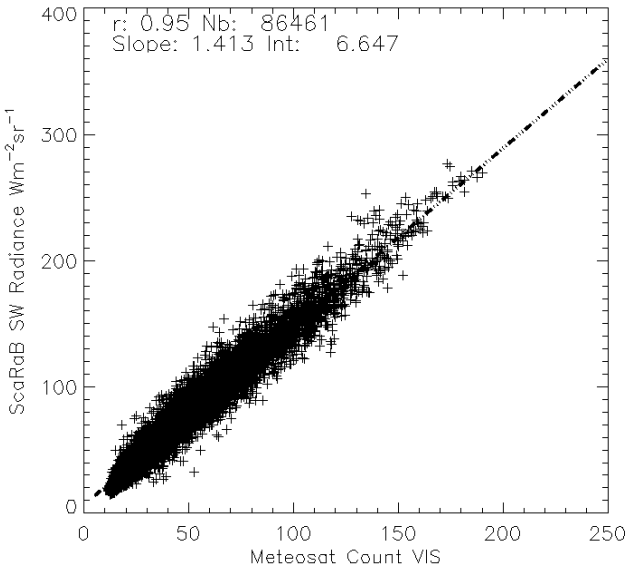

Fig 6 Statistical relationship between the Meteosat count of the 'visible' channel and the SW ScaRaB radiance. The comparison is based on all the matched data for the 50 days of the INDOEX period with only

the solar zenith angle greater than 30° and differences between the Meteosat-ScaRaB viewing zenith angles and relative azimuth angles less than 20°.

3.2.2. Flux Conversion

The radiance comparisons (figure 5) included differences due to angular effects (anisotropy). If these angular effects are properly corrected in the flux computation, the flux regression should theoretically be better. We will see however in this section that the expected improvement is hardy perceptible, as it was already seen by other investigators (M. Vesperini, 1994).

The fluxes from ScaRaB are available in the level 2 product. The flux algorithm first consists in identifying the scene among 5 geotypes and four classes of cloudiness. Then scene-dependent bi-directional functions (Suttles et al, 1988) are used to convert radiance to flux. For METEOSAT flux conversion we use the same ERBE bi-directional function but we classify into the four cloudiness categories according to IR thresholds (293, 283 and 263K).

The flux conversion is applied to the SW estimated radiance of METEOSAT obtained with equation 2. Table 4 shows the regression coefficients between the ScaRaB and METEOSAT estimated flux for three different angular corrections. The first line corresponds to the isotropic model, i.e. radiance x π. (case comparable to Fig 5a). The ERBE ADM has been applied using the ScaRaB scene identification (line 2) and the METEOSAT scene identification (line 3). It can be seen that the ADM improves the correlation, but the difference is subtle. In table 5, the sun glint areas have been rejected. The improvement due to ADM is here almost hidden. The best correlation is finally obtained by eliminating the sun-glint areas (20° angular distance from the specular reflexion) and by averaging the areas over 70x70 km (last column of table 5). The residual rms difference is 41.5 Wm^{-2} and the corresponding scatter plot is shown on figure 7b.

	R
Isotropic case	0.919
ERBE ADM scene id = ScaRaB	0.928
ERBE ADM scene id = from Meteosat IR thresholds	0.929

Table 4 Regression coefficient (R) between the ScaRaB and METEOSAT estimated flux. The METEOSAT averaging area is 47x47 km and the sun glint areas are included. ADM =Angular Dependence Model.

	Glint angle <10°	Glint angle < 20°	same but averaging area =70x70 km
Isotropic case	0.932	0.938	0.950
ERBE ADM scene id = from Meteosat	0.939	0.945 rms=44.55 Wm^{-2}	0.952 rms= 41.5 Wm^{-2}

Table 5. Same as figure 4 but with no sun glint area.

3.3. LW and SW Flux Regressions : summary

These two following (figures 7a and b) summarize the results obtained in comparing the estimated fluxes from ScaRaB and Meteosat. They have been computed with all the collocated observations from January 20th to March 31, about one million for the SW, two millions for the LW. Table 6 contains the statistics corresponding to these figures.

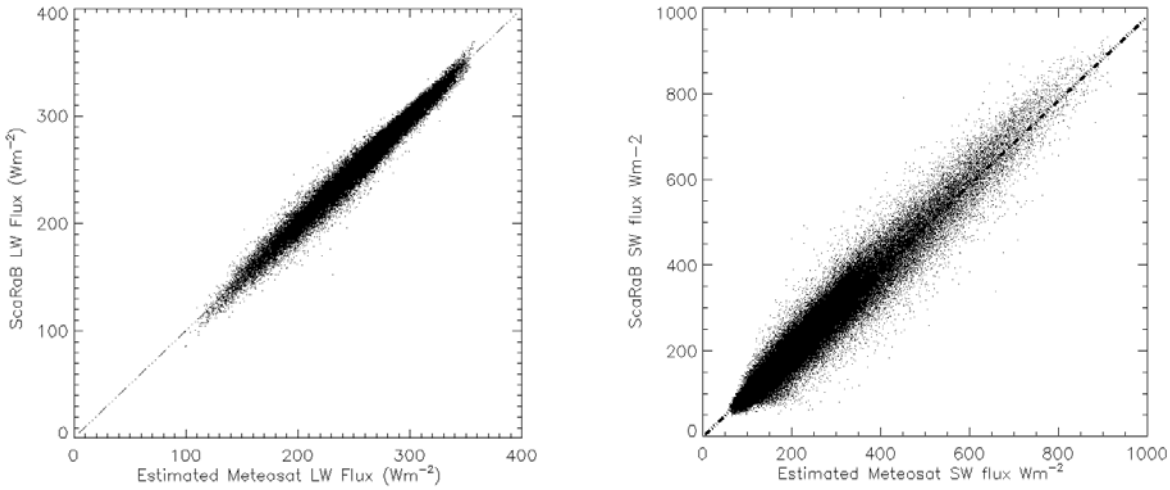

Fig. 7 Statistical relationship between the estimated fluxes from METEOSAT and ScaRaB in the longwave (a) and the shortwave domain (b).

	LW	SW (averaging area 70x70 km)
Slope	0.998	0.982
Intercept	0.545	-1.17
R^2	0.94	0.91
mean residual (Wm^{-2})	9.45	41.4
Number of observations	2 473 344 / 4	1 057 013

Table 6: Statistics corresponding to figure 7.

4. Conclusion

Methods to estimate outgoing fluxes from METEOSAT-5 for the INDOEX experiment have been assessed in the LW and SW domains. In the SW domain the study has dealt with solar zenith angle greater than 60°. The comparisons with ScaRaB estimated fluxes give rms differences of 10 Wm^{-2} and 40 Wm^{-2} respectively, which correspond to results generally found in previous GOES, METEOSAT, ERBE and ScaRaB comparisons. These methods can then be usefully applied to fulfill the gaps between ScaRaB observations.

The results in the SW domain however call some discussions. As pointed by previous studies, the comparison between fluxes is hardly better than between radiances. This is mainly because the flux conversion is applied to a dataset largely noisy. The noise has been generated by errors of collocation and of narrow-to-broadband conversion. When the narrow and broadband measurements come from the same instrument (ScaRaB) or from the same platform (CERES/VIRS or CERES/MODIS) the comparisons show higher correlations (R^2=0.98, rms difference = 20 $W.m^{-2}$ between VIS and SW ScaRaB, R^2=0.99 between averaged VIRS and SW CERES). The correlations can be improved by taken into account different surface covers and zenith solar angles (Li and Trishenko, 1999, Duvel et al., 2000). Since the narrow-to-broadand conversions show only moderate scattering, it can be concluded that the large rms differences observed between the flux estimations from two instruments onboard two different platform mainly come from collocation errors (spatial and temporal mismatches).

For the preparation of the Megha-Tropiques mission, it is suggested this study be improved by reinforcing the co-registration conditions. Collocation may be improved by taking into account the exact ScaRaB footprint or point spread function, or by gridding both data sets. Coincidence between observation pairs may also be improved by reducing the temporal matching to some minutes. Comparisons can also be extended to the METEOSAT-5 2000 data and CERES-TERRA now available (CERES has a better location accuracy than ScaRaB). The interest in having a better co-registration is twofold: it should

- increase the confidence and accuracy of the basic method we have presented here
- allow to use METEOSAT accurate scene-identification to improve ScaRaB flux retrievals in the same way that CERES Edition 2 product use advanced ADM based on imaging radiometers

Obviously the use of data from different platforms cannot challenge perfectly co-registered measurements coming from one unique instrument. However the limits have to be studied to establish the feasibility of the two preceding objectives.

The objectives are pursued in other projects: CERES/TRMM/TERRA/AQUA has already been quoted, GERB will provide broadband radiances on board METEOSAT New Generation (MSG, 2002), POLDER has some unique ability to settle the anisotropy of the SW reflected flux (Loeb et al., 2000, Standfuss and Capderou, 2000)… More generally this study and the ScaRaB/MeghaTropiques project contribute to the efforts in getting reliable flux estimations between different satellite-borne instruments.

5. Acknowledgements

Thanks to the Climserv database (Jean Louis Monge) for making the use of METEOSAT data easier

6. References

Brest C.L., W.B. Rossow and M.D. Roiter, 1997: Update of Radiance Calibrations for ISCCP, *J. Atmos. Oceanic Technol. 14, 1091-1109.*

Cheruy, F., R.S. Kandel and J.P. Duvel, 1991: Outgoing longwave radiation and its diurnal variation from combined ERBE and Meteosat observations. Part II: Using Meteosat data to determine the LW diurnal cycle. J. Geophys. Res., 96, 22623-22630.

Dewitte S., Boekaerts P. and Sirou F, 1999: Determination of the ScaRaB FM1 Broadband Channel Point Spread Functions. *IEEE Transactions on Geoscience and Remote Sensing*, 37, 4, 2004-2010

Duvel, J.-Ph., S. Bouffiès-Cloché and M. Viollier, 2000: Determination of Shortwave Earth Reflectances from visible radiance measurements: Error estimate using ScaRaB data, *J. of Appl. Meteor*, 39, 957-970.

Duvel, J.-Ph., and P. Raberanto, 2000 : A geophysical cross-calibration approach for broadband channels: Application to the ScaRaB experiment, *J. Atmos. Oceanic Technol. 17, 1609-1717.*

Duvel J.P., Viollier M., Raberanto P., Kandel R., Haeffelin M., Pakhomov L.A., Golovko V.A., Mueller J., Stuhlmann R. , and the International ScaRaB Scientific Working Group (ISSWG), 2001, The ScaRaB-Resurs Earth Radiation Budget Dataset and first results, *Bulletin of the American Meterological Society*, 82, 1397-1408.

Haeffelin, M., B. Wielicki, J.-Ph. Duvel, K. Priestley, and M. Viollier, 2001: Intercalibration of CERES and ScaRaB Earth radiation budget datasets using temporally and spatially collocated radiance measurements, *Geophys. Res. Let.*, 28(1), 167-170.

Kandel R., M. Viollier, P. Raberanto, J.Ph. Duvel, L.A. Pakhomov, V.A. Golovko, A.P. Trishchenko, J. Mueller, E. Raschke, R. Stuhlmann, and the International ScaRaB Scientific Working Group (ISSWG), 1998: The ScaRaB Earth Radiation Budget Dataset, *Bulletin of the American Meterological Society*, 79, 765-783.

Loeb N.G., F. Parol, J.C. Buriez and C. Vanbauce, 2000: Top of the atmosphere Albedo Estimation from Angular Distribution Models Using Scene Identification from Satellite Cloud Property Retrievals, Journal of Climate, 1269-1284

Li, Z., and A. Trishchenko, 1999 : A study towards an improved understanding of the relation between visible and SW albedo measurements. *J. Atm. Oc. Technol.*, 17, 347-360.

Li, Z., and A. Trishchenko, 1998 : Synchronous use of GOES and ScaRaB data for studying the Earth's radiation budget and cloud absorption, in *Satellite Remote Sensing of Clouds and the Atmosphere* (ed. J.D. Haigh), *SPIE*, 253-257.

Minnis, P., D.F. Young and E.F. Harrisson, 1991 : Examination of the relationship between outgoing infrared window and total longwave fluxes using satellite data. *J. Climate*, 4, 1114-1133

Roca R., M. Viollier, L. Picon and M. Desbois 2001, 'A multi satellite analysis of deep convection and its moist environment over the Indian Ocean during the Winter Monsoon., *Journal of Geophysical Research*, in press..

Suttles. J.T.. R.N. Green. P. Minnis. G.L. Smith. W.F. Staylor. B.A. Wielicki. I.J. Walker. D.F. Young. V.R. Taylor and L.L. Stowe. 1988: Angular radiation models for Earth-atmosphere system. Volume I - Shortwave radiation. *NASA reference publication 1184*. 144pp.

Standfuss C. and M. Capderou (2000), 'Analysis of Polder Multidirectional radiance measurements for determination of instantaneous reflected shortwave fluxes', *Proceedings of EUMETSAT conference*.

Trishchenko, A., and Z. Li, 1998 : Use of ScaRaB measurements for validating a GOES-based TOA radiation product. *J. Appl. Meteor.,* 591-605

Vesperini M. and Y. Fouquart 1994, 'Determination of broad-band shortwave fluxes from the meteosat visible channel by comparison to ERBE', Beitr. Phys. Atmosph., 67(2):121-132